

## Different strengthening designs and material properties on bending behavior of externally reinforced concrete slab

Saeed Najafi <sup>1a</sup> and Shahin Borzoo <sup>\*2</sup>

<sup>1</sup> Department of Earthquake Engineering, Tarbiat Modares University, Tehran, Iran

<sup>2</sup> Lifeline Earthquake Engineering Department, International Institute of Earthquake Engineering and Seismology, Tehran, Iran

(Received April 23, 2022, Revised September 14, 2022, Accepted September 16, 2022)

**Abstract.** This study investigates the bending behavior of a composite concrete slab roof with different methods of externally strengthening using steel plates and carbon fiber reinforced polymer (CFRP) strips. First, the concrete slab model which was reinforced with CFRP strips on the bottom surface of it is validated using experimental data, and then, using numerical modeling, 7 different models of square-shaped composite slab roofs are developed in ABAQUS software using the finite element modeling. Developed models include steel rebar reinforced concrete slab with variable thickness of CFRP and steel plates. Considering the control sample which has no external reinforcement, a set of 8 different reinforcement states has been investigated. Each of these 8 states is examined with 6 different uncertainties in terms of the properties of the materials in the construction of concrete slabs, which make 48 numerical models. In all models loading process is continued until complete failure occurs. The results from numerical investigations showed using the steel plates as an executive method for strengthening, the bending capacity of reinforced concrete slabs is increased in the ultimate bearing capacity of the slab by about 1.69 to 2.48 times. Also using CFRP strips, the increases in ultimate bearing capacity of the slab were about 1.61 to 2.36 times in different models with different material uncertainties.

**Keywords:** composite FRPs; external reinforcement; reinforced concrete slab; steel deck

### 1. Introduction

Slabs are load-bearing systems that, in addition to the role of bearing gravity loads, transmit the lateral forces that are developed in the floors. Usually, strengthening the bending behavior of the slabs is external with composite or steel materials. The main purpose of this strengthening is reducing the deflection and improving the load capacity of the slab.

In recent years, some studies have been conducted on the behavior of reinforced concrete slabs (Kasu *et al.* 2021, Kim *et al.* 2021, Liang *et al.* 2021, Liao *et al.* 2021, Ramos *et al.* 2021, Tzaros *et al.* 2010). Tzaros *et al.* (2010) developed a numerical model based on non-convex and non-soft optimization to simulate the bending test on two-sided composite concrete slabs with trapezoidal sheets under the slab. They used a numerical model to simulate the experimental procedure and the

---

\*Corresponding author, Ph.D., E-mail: S.borzoo@iiees.ac.ir

<sup>a</sup> Ph.D. Student, E-mail: S.najafi@modares.ac.ir

capacity of the slab in the form of diagrams was compared. Also, the results were obtained by a numerical procedure using non-smooth energy optimization theory compared with experimental testing (Tzaros *et al.* 2010).

Hedaoo *et al.* (2012) reviewed and compared experimental and numerical models in composite steel deck slabs. They evaluated the interaction of concrete and steel deck using shear studs to modify shear bond characteristics. Also, an analytical evaluation of longitudinal shear bond strength between the concrete and steel deck with partial shear connection was carried out. Their experimental output and analytical results of composite slabs revealed good agreements (Hedaoo *et al.* 2012). Mamede *et al.* (2013) worked on the cutting of flat concrete slabs which contain oblique steels in experimental and 3D analytical models. Their analytical model was developed in Atena 3D software with a parametric analysis mode, and different models were created by changing the dimensions of the slab and column elements (Mamede *et al.* 2013). Genikomsou and Polak (2015) studied the finite element analysis of the punching shear in concrete slabs using the plastic damage model in ABAQUS software. Their model was a slab attached to a column. Eldib *et al.* (2009) worked on the modeling and analysis of two-sided composite slabs, using Cosmos software with non-linear properties of the material. Their finite element model was validated by full-scale tests of two-way composite slabs. The effect of cold-formed steel strips, variation of its thickness and distribution, effect of shear studs, and the effect of the mentioned parameters on the ultimate capacity and slab deflection are investigated. Results of their study showed a considerable decrease in slab deflection by using steel strips and studs (Eldib *et al.* 2009).

In recent years, a lot of research has been done on reinforcing concrete slabs with composite materials. Teng and Zhang (2014) worked on a reinforced concrete slab strengthened with Fiber-reinforced plastic (FRP) using the finite element method. In this study, they used a plate element to cover the bottom of the slab to model the composite layer (Teng and Zhang 2014). In 2016, Feng *et al.* investigated the flexural behavior of reinforced concrete slabs with a mesh plate made of composite materials. This lattice plate covers the entire bottom of the concrete slab and acts somewhat similar to the slab mold (Fang *et al.* 2016). Feng *et al.* investigated the bending behavior of reinforced concrete slabs using FRP boards. FRP reinforced concrete slab grid face sheets (CFGF) are a new form of structural member. In this type of slab, the combination of FRP and concrete are used to obtain several advantages. CFGF may be built on-site or prefabricated. FRP grid and slab face act as reinforcement when the slab is bent. The section transformation method was used to evaluate the overall bending stiffness and transverse deflection of CFGF. A comparison between experimental results and analytical modeling showed that this method accurately predicts the bending stiffness as well as the final capacity of the slab (Fang *et al.* 2016).

Abdul-Salam *et al.* (2016) investigated the shear strength of one-way FRP-reinforced slabs. The shear behavior of reinforced concrete with FRP without web reinforcement is potentially one of the most important cases due to the fragile nature of concrete. In this research, a total of 16 samples of one-way concrete slabs with glass and carbon fiber reinforced polymer (CFRP) rebars in presence of steel reinforcement have been made and tested until failure under four-point bending loading. The experimental results confirmed that the axial stiffness of longitudinal FRP reinforcement on shear strength is effective. Most of the CFRP-reinforced slabs experienced fragile failure, while many GFRP-reinforced slabs with axial stiffness equal to those with CFRP-reinforced slabs had their stability even after failure and fragile failure modes were avoided (Abdul-Salam *et al.* 2016).

In this paper different models of reinforced concrete slabs using CFRP strips and steel plates are developed and compared.

## 2. Methodology

To validate the developed finite element model, the experimental study by Agbossou *et al.* (2008) is used. At the Savoy University of Technology, Agbossou *et al.* (2008) constructed four reinforced concrete slabs in size of  $1.25 \times 1.25 \times 0.1$  m in an experimental study. Their reinforced slabs are strengthened by FRP layers. In their study, the compressive strength of the used concrete is 36 MPa and its tensile strength is 3.3 MPa. The reinforced steel in this study is ST 65C with welded mesh type ( $A = 636 \text{ mm}^2$ ,  $s = 100 \times 100$ ,  $\phi_s = 9 \text{ mm} \times 9 \text{ mm}$ ) for the lower side and ST 35C ( $A = 385 \text{ mm}^2$ ,  $s = 100 \times 100$ ,  $\phi_s = 7 \text{ mm} \times 7 \text{ mm}$ ) for the upper side. The minimum cover of the rebars is 25 mm and the steel grid is completely in the middle of the concrete slab. The CFRP with a dimension of  $50 \times 150 \times 1$  mm thick was used. These fibers are glued to the bottom surface of the concrete slab after cleaning. The concrete slab was placed in 4 directions with a length of 1.2 meters on simple supports at its edges. A hydraulic jack with a capacity of 500 kN was used to apply the load locally on a surface with a dimension of 10 by 10 cm in the center of the slab. The load and displacement of steel along with composite strains are measured using gauges during the loading of the slab.

### 2.1 Analytical modeling

For analytical models, a slab with a thickness of 10 cm and dimensions of 125 by 125 cm has been used. The slab model is developed with two crossing CFRP reinforcement strips at the bottom of it. The solid extrude part and planner shell is used to create concrete and CFRP strips respectively. The steel rebar reinforcement is created using wire and truss elements. The isotropic elastic and plastic properties are considered for steel materials. For concrete material elastic property has been used and also to define the occurrence of cracks in the cross-section, the concrete smeared cracking method has been used.

To model the used composite material in the validated model, due to the different modules of elasticity of the composite reinforcing strips in two directions, the properties of the lamina are chosen and its module of elasticity according to the values that are shown in Table 1 which has been adopted from Agbossou *et al.* (2008).

To define the interaction between steel rebar reinforcement and concrete, the interaction module and the embedded region constraint is adopted. The applied load on the center of the slab is shown in Fig. 1.

To model the supports, a rigid element in the form of a square frame with internal dimensions of 120 by 120 cm and external dimensions of 126 by 126 cm has been used and the concrete slab is placed on this square rigid frame (Fig. 2). In this study, the dimensions of the mesh are selected equal to 2.5 cm, which has been adopted by using sensitivity analysis and repeated reduction of mesh sizes with trial and error and finally convergence of the responses.

In this research, for analyzing models, the type of static general analysis is used. To define the contact in the interaction module, tangential behavior with rough friction and normal behavior with hard contact are selected. Also, interaction is defined as surface-to-surface contact. Also, the shell

Table 1 Specifications of used composite materials (FRP) in the validation model

E1 (Mpa)	E2 (Mpa)	Nu12	G12 (Mpa)	G13 (Mpa)	G23 (Mpa)
100750	1007.5	0.22	3270	3270	1860

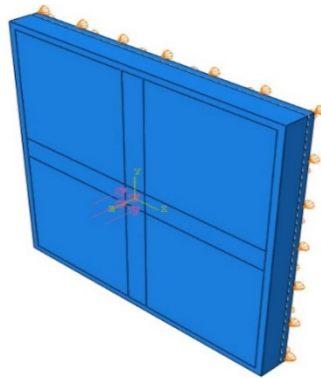


Fig. 1 Applied load on the slab and boundary condition according to Agbossou *et al.* (2008)

to solid constraint is used to define the contact between CFRP strips and concrete. Moreover, to define the interactions between steel rebars and concrete, the embedded region constraint is used. Force versus displacement diagrams for verification of the numerical model is presented in Fig. 3.

The concrete smeared cracking method, to define the failure surface of the concrete is selected. Table 2 shows the parameters introduced in ABAQUS software for modeling concrete properties.

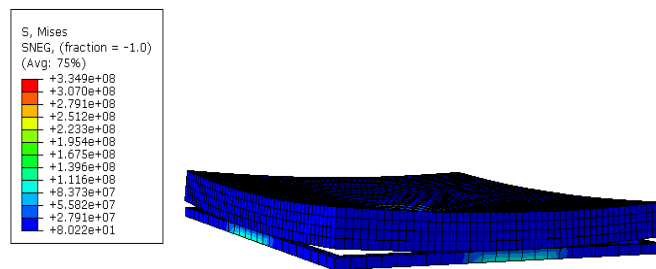


Fig. 2 The finite element model of concrete slab based on the experimental model with square a rigid frame (Agbossou *et al.* 2008)

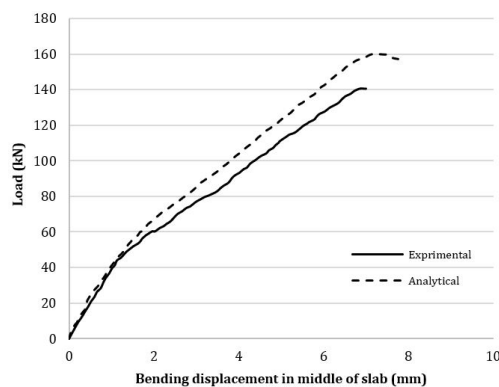


Fig. 3 Comparison of the results of the numerical model and the experimental model of Agbossou *et al.* (2008)

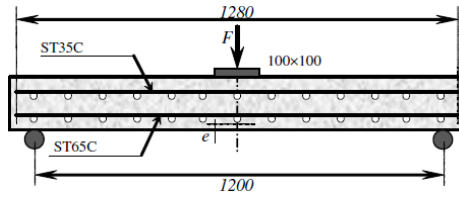


Fig. 4 Loading and specifications of the experimental model (Agbossou *et al.* 2008)



Fig. 5 Experimental slab model under loading (Agbossou *et al.* 2008)

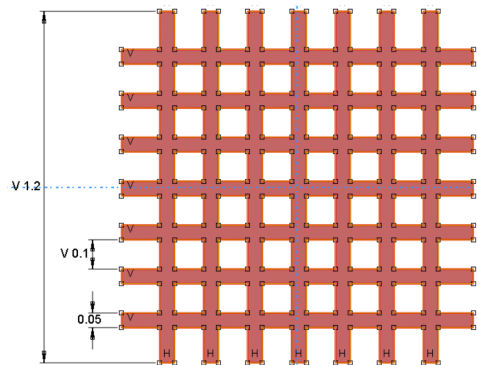


Fig. 6 CFRP strips geometry and dimensions

Table 2 Specifications of concrete materials (concrete smeared cracking)

Concrete smeared cracking model		Failure ratios		Tension stiffening	
Compressive stress (Mpa)	Plastic strain	Ratios	Assigned value	Sigma/sigma-c	Epsilon/epsilon-c
24.09	0	Ratio 1	1.18	1	0
29.2	0.0004	Ratio 2	1	0	0.0005
31.7	0.0008	Ratio 3	1.25		
32.35	0.0012	Ratio 4	1		
31.76	0.0016				
30.37	0.002				
28.5	0.0024				
21.9	0.0036				

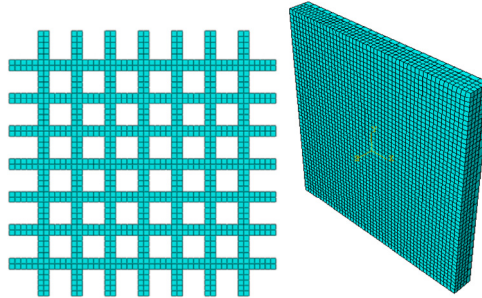


Fig. 7 Meshing of the analytical model

Elements 3D stress C3D8R with 8 nodes linear brick, reduced integration, and hourglass control are used for meshing concrete slabs. Also, for meshing CFRP strips, truss element T3D2 with 2 nodes linear 3D truss is used.

As mentioned, a total of 8 types of the slab with different external reinforcements are investigated. For each slab, 6 different uncertainties in rebar and concrete ultimate strength are selected. Hence, 48 analytical models are evaluated in the present study. These 8 models include two concrete slabs with CFRP reinforcement materials, 5 types of variable steel decks, and a slab without any reinforcement as a control model. Models 1 and 2 are reinforced with CFRP composite material with a thickness of 0.1 mm, and 0.2 mm respectively. Model 3 has no kind of external reinforcement and models 4, 5, 6, 7 and 8, in addition to the upper and lower steel rebar reinforcements, contain 1 mm, 2 mm, 3 mm, 4 mm, and 5 mm steel plates attached to the bottom face of the slab to increase the ductility and reduce the brittle behavior of the concrete. The load is applied to the models until the failure. To compare the behavior of different samples and determine the effect of using steel sheets on the slab, force-displacement diagrams are presented.

In Table 4, based on the different compressive strengths of concretes and the ultimate tensile strength of rebars, 6 different series of specifications for 8 different mentioned reinforcing for slabs are developed.

Table 3 Specifications of seven types of modeled slabs with different external reinforcement

Model no	External reinforcement
1	CFRP 0.2 mm
2	CFRP 0.1 mm
3	Without external reinforcement
4	PL 1 mm
5	PL 2 mm
6	PL 3 mm
7	PL 4 mm
8	PL 5 mm

Table 4 Specifications of each series in different models

Series number	$F_u(kg/cm^2)$ of steel rebars	$f'_c(kg/cm^2)$
1	4000	210
2	5000	210
3	4000	240
4	5000	240
5	4000	280
6	5000	280

### 3. Results and discussion

In this section, firstly, graphic outputs which are related to numerical models are presented. Due to the multiplicity of the models, only a part of these outputs is provided for each of the different cases. Fig. 8 shows the plastic strains created in slab steel rebar reinforcements. As can be seen, the

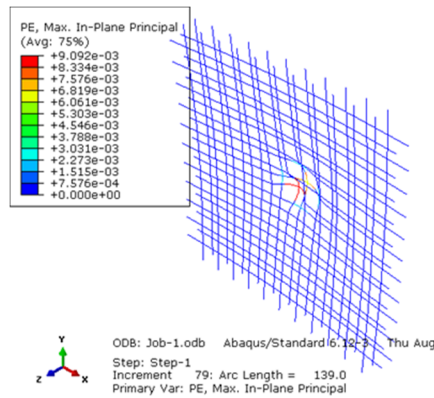


Fig. 8 Plastic strains in steel rebar reinforcements

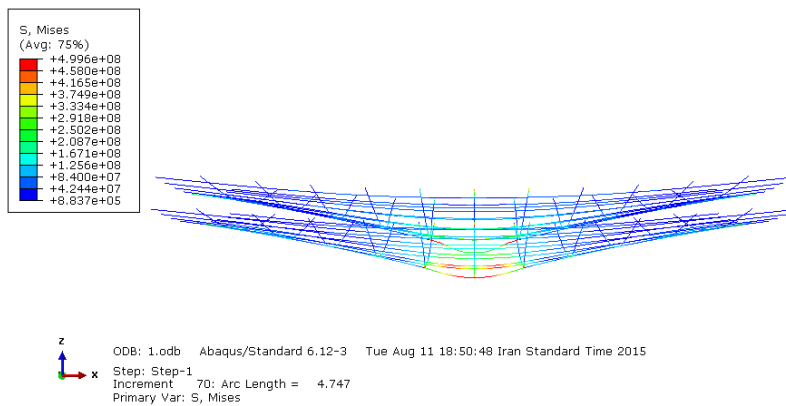


Fig. 9 Stresses in the upper and lower rebars of model 1

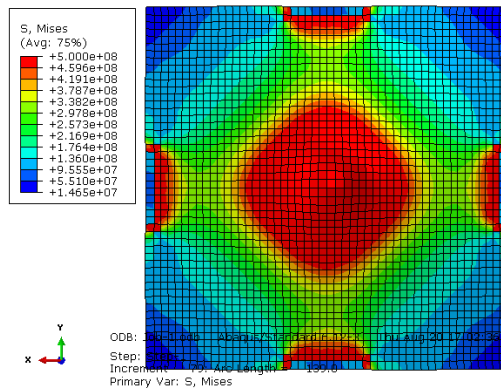


Fig. 10 Stress values generated in the steel plate

maximum values of the strain of the reinforcements are at the location of the applied load. This indicates that after the occurrence of small cracks in the concrete and the expansion of cracks by applying more loads, concrete eventually would fail at a specific point and after that, rebars will resist the load. Fig. 9 shows the stresses which are produced in the upper and lower rebars of model 1. Fig. 9 indicates the displacement and stresses created in steel rebars. This figure shows that displacement and stress of slab rebars have their maximum values at the center of it where the load is applied. The stresses in rebars are reduced by moving away from this area to slab supports.

Fig. 10 shows the stresses produced in the steel sheet under the slab. As can be seen, the stresses in the steel sheet are different from the stresses in the rebars. As it was seen in the rebars with moving away from the center of the slab where the load is applied, the stresses are reduced, but in the steel sheet, in addition to the center of the sheet, four stress concentration points are also observed at the four points, where the plate is in contact with the rigid support frame.

Fig. 11 shows the displacements in the concrete slab. As can be seen in this figure, after applying the load until the failure occurrence, the corner displacement is upwards.

### 3.1 Results of the externally reinforced models using CFRP with a thickness of 0.1 and 0.2 mm

In this section, the results of two reinforced models with CFRP are compared in the form of force-displacement curves. Each diagram is related to a separate type of external reinforcement,

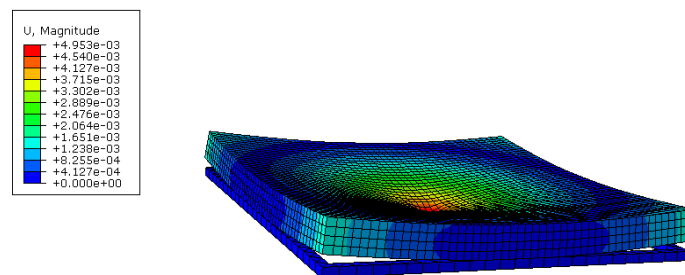


Fig. 11 Deformation in the validation model



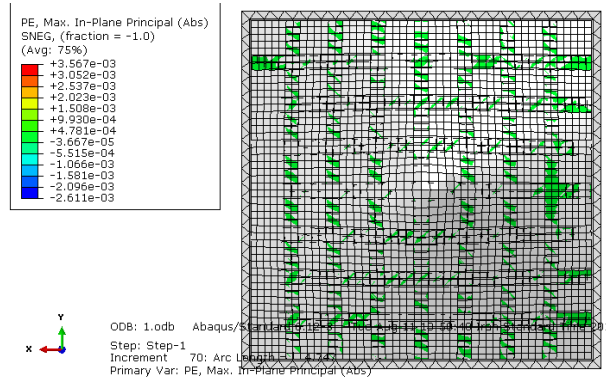


Fig. 12 Plastic strain in CFRP strips of validation model

which consists of six different series due to uncertainties related to concrete and steel materials.

From Fig. 13 it can be concluded that below the about 2 cm displacement at the center of the slab, in the exact place of applied load, the inherent characteristics of concrete and steel have little effect on the load-bearing capacity of the slab. However, the high strength of concrete has shown its effect on maximum load-bearing capacity. For example, for series 6 with a compressive strength of 280 Mpa, the maximum amount of load-bearing capacity has been increased to a specified point. Finally, after cracking of the concrete, which occurred in a displacement of about 2.5 cm for series 6, then composite materials would resist the load, and the force-displacement diagram becomes a straight line, which continues to increase with increasing load.

As it can be seen from Figs. 13 and 14 the force-displacement of the applied load point for models with 0.1 and 0.2 mm CFRP are the same as each other in behavior and form. The main characteristic of these models is an approximately linear increase of force until occurring complete failure. The amount of increased intolerable force with increasing CFRP thickness is negligible, this indicates that increasing the thickness of composites to improve bearing capacity will not be very practical.

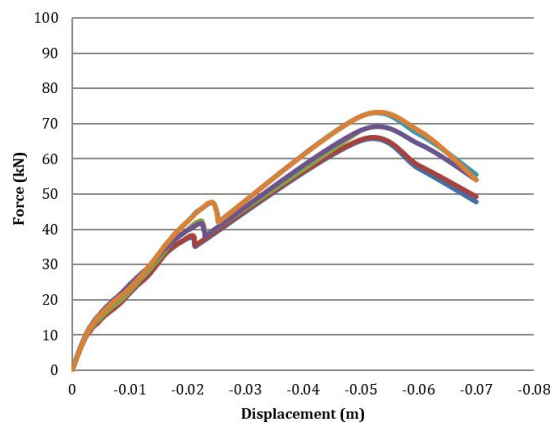


Fig. 13 Force-displacement of applied load point in the center of the slab for models with 0.1 mm CFRP

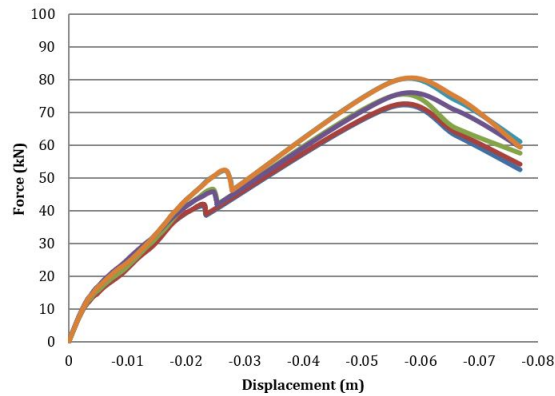


Fig. 14 Force-displacement of applied load point in the center of the slab for models with 0.2 mm CFRP

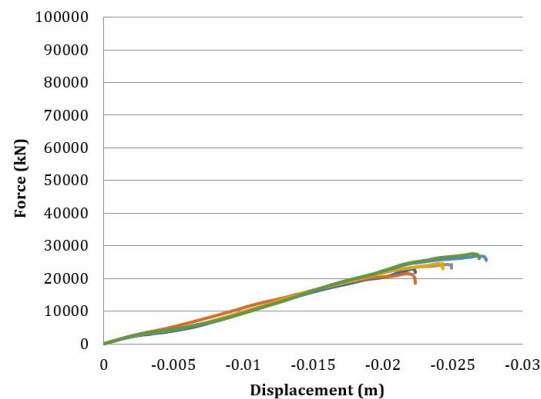


Fig. 15 Force-displacement of applied load point in the center of the slab for models without steel sheet

### 3.2 Results of the models without externally reinforced steel plates

In this case, no other material has been used to strengthen the slab, and only reinforced concrete with two layers of lower and upper steel rebar reinforcement is used. In these models, when the reinforced slab concrete reaches its ultimate strength, it no longer has much resistance to the applied force. Moreover, the force-displacement diagram is significantly reduced and it is also clear that the final strength of the rebars does not have much effect on increasing the load-bearing capacity of the slab, and the samples with stronger concrete have shown more resistance to the load.

### 3.3 Results of the externally reinforced models with the steel plate with a thickness of 1 or 2 mm

In models with steel plates attached at the bottom of reinforced concrete slabs, the strength of concrete and rebars, as well as steel sheets, have little effect on increasing the load-bearing capacity of concrete slabs. Hence, the force-displacement diagrams are generally in a close range and their flexural behavior is similar to each other. It is concluded that the effect of increasing the strength of

concrete, in this case, is greater than the effect of increasing the ultimate strength of the rebar. It is also observed that when the plate is used uniformly on the bottom of the slab, more load-bearing capacity is obtained due to the combined performance of the concrete slab and steel plate than the use of composite materials. The only difference is that, with increasing displacement, the force-displacement diagram becomes horizontal and there is no increase in the amount of the force after concrete cracking. As shown before, in presence of composite materials, due to their high tensile strength, the force-displacement diagram continues linearly with a high slope after the concrete cracks.

From Figs. 16 and 17, it is comprehended that force-displacement of applied load points for models with 1 and 2 mm steel plates are the same in behavior and format. Unlike models with CFRP, the force-displacement curves of these models are approximately horizontal after occurring initial cracks in concrete. It can be seen that the amount of the increased intolerable force with increasing steel plate thickness is negligible, so increasing the thickness of the steel plate to improve the flexural behavior of the slab would not be very efficient.

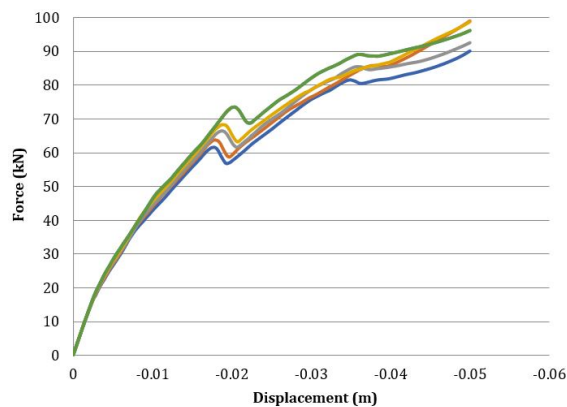


Fig. 16 Force-displacement of applied load point in the center of the slab for models with the 1 mm steel sheet

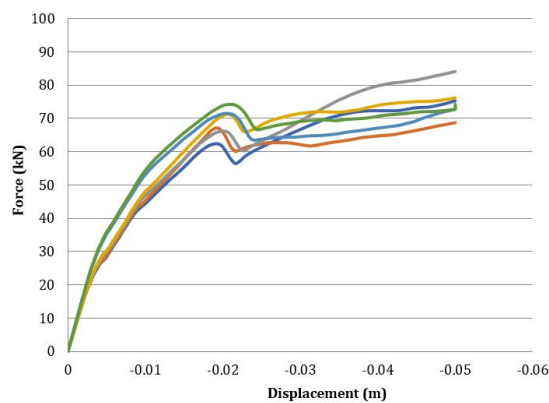


Fig. 17 Force-displacement of applied load point in the center of the slab for models with the 2 mm steel sheet

### 3.4 Results of the externally reinforced models with the steel plate with a thickness of 3 mm

According to the force-displacement diagrams, it can be seen that when a 3 mm thick steel plate is used to strengthen the concrete slab, the effect of uncertainties related to the strength of concrete and rebars are significant. The steel sheets also increase the initial stiffness of the system with increasing displacement. It is found that the effect of increasing the strength of concrete, in this case, is greater than the effect of increasing the final strength of the rebars. It is also observed that when the plate is used uniformly on the bottom of the slab, less load-bearing capacity is obtained for the combined performance of the concrete slab and steel sheet than the use of composite materials. It should be noted that the final strength of the slab against the load does not always increase by increasing the thickness of the steel plate. In Fig. 18 it is obvious that from a specific displacement onwards, the diagram shows a decrease in force values and becomes horizontal. For the model with the 3 mm steel plate, it happens in a displacement of about 2.5 cm and we will no longer witness an increase in the amount of load after that. But as was seen before the composite materials, due to their high tensile strength had a linear increase of tolerable force with a relatively steep slope after the concrete cracks and breaks.

### 3.5 Results of the externally reinforced models with the steel plate with a thickness of 4 mm

Fig. 19 implies that increasing the thickness of the steel sheet does not always have a positive effect on increasing the strength of the concrete slab against displacement. This happens because, although increasing the thickness of the steel plate the strength of the composite slab increases to a certain point, from then it will not have much effect on improving the slab performance. Because increasing the thickness of the steel sheet more than a certain limit, makes the combined performance of the concrete slab and the steel plate will not happen. In this research, it was revealed that 1 mm thickness is very useful than any other model and no more increase would be necessary. This stems from the fact that when loads are applied on the slab the steel sheet does not have any deformation due to its thickness, while the concrete is crushed in the range of applied loads and loses its strength.

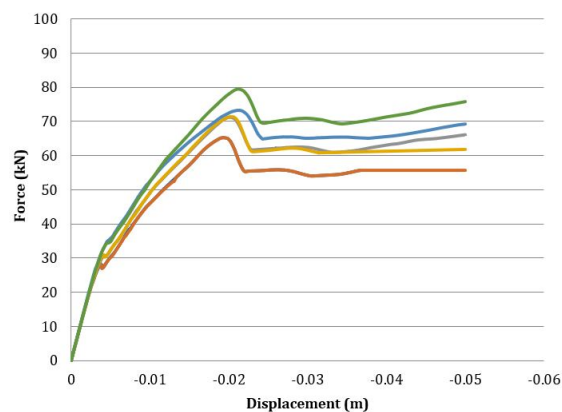


Fig. 18 Force-displacement of applied load point in the center of the slab for models with the 3 mm steel sheet

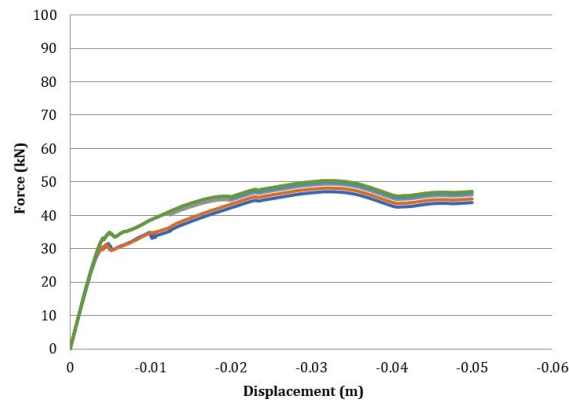


Fig. 19 Force-displacement of applied load point in the center of the slab for models with 4 mm steel sheet

Therefore, as can be seen from the force-displacement diagrams in Fig. 19, the slope of the initial part of the diagrams is much higher than in the previous cases, which is due to the high stiffness of the steel sheet under the concrete slab, but the mechanism of composite effect does not activate in these cases.

### 3.6 Results of the externally reinforced models with the steel plate with a thickness of 5 mm

From the observation of Figs. 19 and 20, it is concluded that the same results of using the 4 mm plate are concluded replacing it with a 5 mm thickness and it is clear that increasing the thickness of a steel sheet does not always have a positive effect on increasing the strength of composite concrete slabs. Moreover, it is particularly noticeable that in this case, the significant impact of concrete compressive strength on the strength of the concrete slab is steel obvious, so the concrete diagrams with a strength of 280 are higher than the rest of the samples.

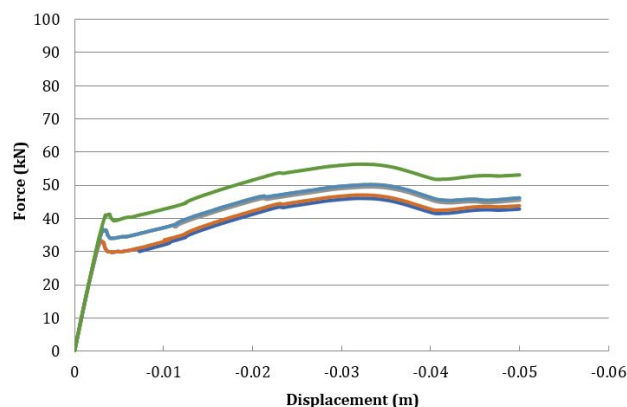


Fig. 20 Force-displacement of applied load point in the center of the slab for models with a 5 mm steel sheet

Table 5 Comparing the maximum recorded displacement and strength of each model

External reinforcing		Series					
		1	2	3	4	5	6
CFRP 0.2 mm	Max disp (m)	-0.07	-0.07	-0.07	-0.07	-0.07	-0.07
	Max force (kN)	71.6	71.8	74.9	74.8	79.1	79.2
CFRP 0.1 mm	Max disp (m)	-0.07	-0.07	-0.07	-0.07	-0.07	-0.07
	Max force (kN)	65.1	65.4	68.1	68.1	72.0	72.0
Without bounding	Max disp (m)	-0.022	-0.022	-0.025	-0.024	-0.027	-0.027
	Max force (kN)	22.9	21.3	24.2	24.4	26.9	27.6
PL 1 mm	Max disp (m)	-0.05	-0.05	-0.05	-0.05	-0.05	-0.05
	Max force (kN)	90.1	99.0	92.5	98.7	96.1	96.1
PL 2 mm	Max disp (m)	-0.05	-0.05	-0.05	-0.05	-0.05	-0.05
	Max force (kN)	75.2	68.7	84.0	76.1	72.7	74.2
PL 3 mm	Max disp (m)	-0.037	-0.05	-0.05	-0.05	-0.05	-0.05
	Max force (kN)	65.2	65.2	71.2	71.3	73.2	79.4
PL 4 mm	Max disp (m)	-0.05	-0.05	-0.05	-0.05	-0.05	-0.05
	Max force (kN)	47.0	48.1	49.3	50.3	54.0	56.3
PL 5 mm	Max disp (m)	-0.05	-0.05	-0.05	-0.05	-0.05	-0.05
	Max force (kN)	46.0	47.0	49.4	50.2	54.2	56.3

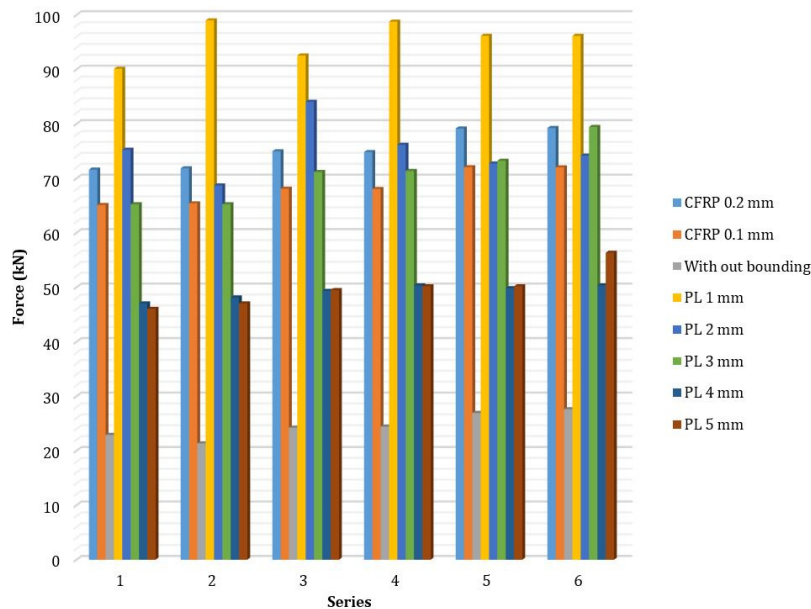


Fig. 21 Comparing the maximum load capacity of each model

Table 5 shows the maximum displacement values and the maximum force for each model. As can be seen, series 1 to 6 are provided for each external reinforcement model.

Fig. 21 shows the amount of bearing force by each model. As shown in this figure, the model with 1 mm plate reinforcement has the highest load-bearing capacity. After this, the CFRP composite reinforcement models with 0.2 mm thickness and the next CFRP composite reinforced models with 0.1 mm thickness have the highest recorded force. Contrary to the first belief, increasing the reinforcement steel plate under the slab is not directly affecting increasing the strength of the reinforced concrete slab. So, with increasing the thickness of the steel sheet, the strength of the reinforced slab has decreased. According to the results, it is felt that increasing the steel sheet is not a good and economical solution to increase the strength of the slab, although all reinforced models have more strength than the control model which was without reinforcement.

Table 6 shows the values of increasing the strength of the slab in terms of percentage. As can be seen, models which are reinforced using a steel plate with more than 2 mm thickness have the lowest

Table 6 Comparing the effect of external reinforcement in increasing the ultimate strength % for different models

Series	CFRP 0.2 mm	CFRP 0.1 mm	PL 1 mm	PL 2 mm	PL 3 mm	PL 4 mm	PL 5 mm
1	2.13	1.84	2.93	2.29	1.85	1.05	1.01
2	2.36	2.06	3.64	2.22	2.06	1.25	1.20
3	2.09	1.81	2.82	2.47	1.94	1.04	1.04
4	2.06	1.79	3.04	2.12	1.92	1.06	1.05
5	1.94	1.67	2.57	1.70	1.72	1.01	1.01
6	1.87	1.61	2.48	1.69	1.88	1.04	1.04

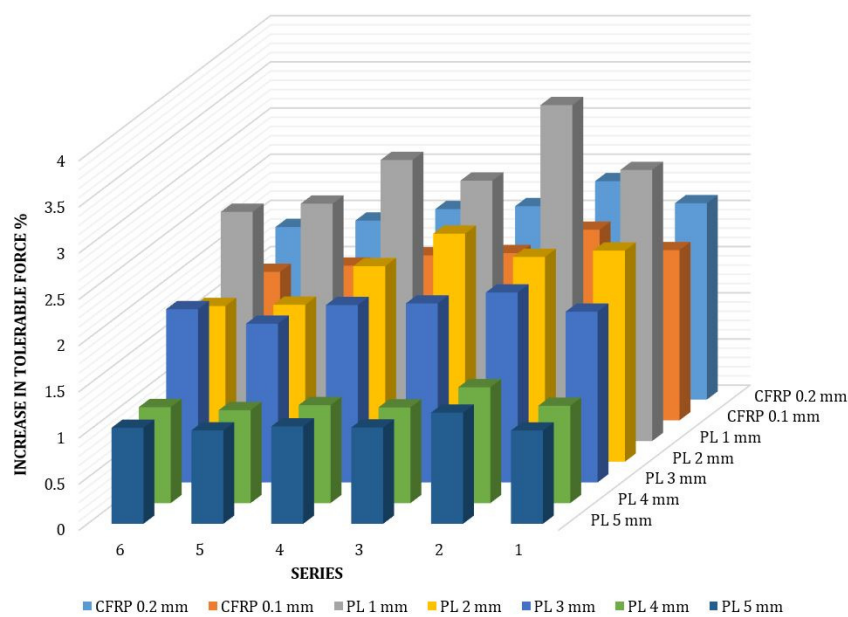


Fig. 22 Comparing the effect of external reinforcement on the load-bearing capacity of each model

increase. Considering terms of uncertainty related to the materials, negligible changes are observed in increasing the strength and decreasing the displacement, which indicates that the effect of increasing the characteristic strength of concrete or the resistance of rebars to external reinforcement is very insignificant. The results show that most of the increases are related to series 2 in all cases. This shows that in designing slabs, to achieve the highest strength, the concrete specified strength characteristic has less effect than increasing the ultimate stress of steel rebars. It was observed that although the existence of steel plates improves the flexural behavior of composite slabs, a further increase in the thickness of the plate by more than 1 mm would not be necessary. In models with 1 and 2 mm steel plates the maximum strength and ultimate strength of the slab increased, but then for the model with 3, 4, and 5 mm steel sheets, the high stiffness of the sheet and its incompatible performance with the concrete slab, caused poor performance of the composite roof system.

Fig. 22 demonstrates in all models where the final stress of the rebars is increased and the characteristic strength of concrete is constant, better results have been observed in increasing the strength of the slab.

#### 4. Conclusions

In this paper, a concrete slab with different methods of strengthening and different properties of materials is modeled. A general comparison of the force-displacement diagrams shows that the ultimate tensile strength of the rebars in investigated models has little effect on increasing the strength of concrete against the applied load. Also, the effect of the compressive strength of concrete on the final load-bearing capacity of the slab is noticeable. In the models with a steel plate, it can be mentioned that increasing the thickness of the steel plate at the bottom of the slab up to a determined threshold thickness increases the strength of the composite slab and from then on, it will not have much effect on further improving the slab performance. It observed that although the existence of steel plates improves the flexural behavior of composite slabs, a further increase in the thickness of the plate by more than 1 mm would not be necessary.

In models with 1 and 2 mm steel plates the maximum strength and ultimate strength of the slab increased, but then for the model with 3, 4, and 5 mm steel sheets, the high stiffness of the sheet and its incompatible performance with the concrete slab, caused poor performance of the composite roof system. Also, it concluded that though the initial stiffens and results of the force-displacement curves for the composite concrete slab with the metal deck in small displacements are higher but the cases reinforced with composite materials (CFRP) behave much better in flexural actions.

#### References

- Abdul-Salam, B., Farghaly, A.S. and Benmokrane, B. (2016), "Mechanisms of shear resistance of one-way concrete slabs reinforced with FRP bars", *Constr. Build. Mater.*, **127**, 959-970. <https://doi.org/10.1016/j.conbuildmat.2016.10.015>
- Agbossou, A., Michel, L., Lagache, M. and Hamelin, P. (2008), "Strengthening slabs using externally-bonded strip composites: Analysis of concrete covers on the strengthening", *Compos. Part B: Eng.*, **39**(7-8), 1125-1135. <https://doi.org/10.1016/j.compositesb.2008.04.002>
- Eldib, M.E.A.H., Maaly, H.M., Beshay, A.W. and Tolba, M.T. (2009), "Modelling and analysis of two-way composite slabs", *J. Constr. Steel Res.*, **65**(5), 1236-1248. <https://doi.org/10.1016/j.jcsr.2009.01.002>
- Fang, H., Xu, X., Liu, W., Qi, Y., Bai, Y., Zhang, B. and Hui, D. (2016), "Flexural behavior of composite concrete slabs reinforced by FRP grid facesheets", *Compos. Part B: Eng.*, **92**, 46-62.



- <https://doi.org/10.1016/j.compositesb.2016.02.029>
- Genikomsou, A.S. and Polak, M.A. (2015), "Finite element analysis of punching shear of concrete slabs using damaged plasticity model in ABAQUS", *Eng. Struct.*, **98**, 38-48.  
<https://doi.org/10.1016/j.engstruct.2015.04.016>
- Hedao, N.A., Gupta, L.M. and Ronghe, G.N. (2012), "Design of composite slabs with profiled steel decking: a comparison between experimental and analytical studies", *Int. J. Adv. Struct. Eng.*, **4**(1), 1-15.  
<https://doi.org/10.1186/2008-6695-3-1>
- Kasu, S.R., Tangudu, J., Chandrappa, A.K. and Reddy, M.A. (2021), "Influence of stiffness of dry lean concrete base on load stresses in the plain cement concrete slab of concrete pavements", *Road Mater. Pave. Des.*, **23**(8), 1942-1955. <https://doi.org/10.1080/14680629.2021.1924237>
- Kim, H.-Y., You, Y.-J., Ryu, G.-S., Ahn, G.-H. and Koh, K.-T. (2021), "Concrete slab-type elements strengthened with cast-in-place carbon textile reinforced concrete system", *Materials*, **14**(6), 1437.  
<https://doi.org/10.3390/ma14061437>
- Liang, H., Xie, W., Wei, P., Zhou, Y. and Zhang, Z. (2021), "The effect of the decorative surface layer on the dynamic properties of a symmetric concrete slab", *Symmetry*, **13**(7), 1174.  
<https://doi.org/10.3390/sym13071174>
- Liao, W., Zeng, C., Zhuang, Y., Ma, H., Deng, W. and Huang, J. (2021), "Mitigation of thermal curling of concrete slab using phase change material: A feasibility study", *Cement Concrete Compos.*, **120**, 104021.  
<https://doi.org/10.1016/j.cemconcomp.2021.104021>
- Mamede, N.F.S., Ramos, A.P. and Faria, D.M. (2013), "Experimental and parametric 3D nonlinear finite element analysis on punching of flat slabs with orthogonal reinforcement", *Eng. Struct.*, **48**, 442-457.  
<https://doi.org/10.1016/j.engstruct.2012.09.035>
- Mou, B., Zhao, F., Wang, F. and Pan, W. (2021), "Effect of reinforced concrete slab on the flexural behavior of composite beam to column joints: Parameter study and evaluation formulae", *J. Constr. Steel Res.*, **176**, 106425. <https://doi.org/10.1016/j.jcsr.2020.106425>
- Ramos, A., Correia, A.G., Calçada, R., Costa, P.A., Esen, A., Woodward, P.K., Connolly, D.P. and Laghrouche, O. (2021), "Influence of track foundation on the performance of ballast and concrete slab tracks under cyclic loading: Physical modelling and numerical model calibration", *Constr. Build. Mater.*, **277**, 122245. <https://doi.org/10.1016/j.conbuildmat.2021.122245>
- Soufeiani, L., Ghadyani, G., Kueh, A.B.H. and Nguyen, K.T.Q. (2017), "The effect of laminate stacking sequence and fiber orientation on the dynamic response of FRP composite slabs", *J. Build. Eng.*, **13**, 41-52. <https://doi.org/10.1016/j.job.2017.07.004>
- Teng, X. and Zhang, Y.X. (2014), "Nonlinear finite element analyses of FRP-strengthened reinforced concrete slabs using a new layered composite plate element", *Compos. Struct.*, **114**, 20-29.  
<https://doi.org/10.1016/j.compstruct.2014.03.040>
- Tzaros, K.A., Mistakidis, E.S. and Perdikaris, P.C. (2010), "A numerical model based on nonconvex-nonsmooth optimization for the simulation of bending tests on composite slabs with profiled steel sheeting", *Eng. Struct.*, **32**(3), 843-853. <https://doi.org/10.1016/j.engstruct.2009.12.010>